Cellular and network mechanisms of rhythmic recurrent activity in neocortex

Maria V. Sanchez-Vives[1,2] and David A. McCormick[1]

[1] *Section of Neurobiology, Yale University School of Medicine, 333 Cedar Street, New Haven, Connecticut 06510, USA*

[2] *Present address: Instituto de Neurociencias UMH-CSIC, Apartado 18, 03550 San Juan de Alicante, Spain*

Correspondence should be addressed to D.A.M. (david.mccormick@yale.edu)

The neocortex generates periods of recurrent activity, such as the slow (0.1–0.5 Hz) oscillation during slow-wave sleep. Here we demonstrate that slices of ferret neocortex maintained *in vitro* generate this slow (< 1 Hz) rhythm when placed in a bathing medium that mimics the extracellular ionic composition *in situ*. This slow oscillation seems to be initiated in layer 5 as an excitatory interaction between pyramidal neurons and propagates through the neocortex. Our results demonstrate that the cerebral cortex generates an 'up' or depolarized state through recurrent excitation that is regulated by inhibitory networks, thereby allowing local cortical circuits to enter into temporarily activated and self-maintained excitatory states. The spontaneous generation and failure of this self-excited state may account for the generation of a subset of cortical rhythms during sleep.

The cerebral cortex is constantly active. Even during slow-wave sleep, cortical and subcortical networks interact to generate rhythmic patterns of activity at a variety of frequencies[1–4], including a 'slow rhythm' characterized by the recurrence of tonic activity in cortical neurons approximately once every three to five seconds[2–9]. This slow oscillation is generated within the neocortex and may coordinate other sleep rhythms (such as spindle waves and delta waves) into a coherent rhythmic sequence of recurring cortical and thalamocortical activities[2–5]. The slow oscillation is associated with the arrival of a relatively steady barrage of excitatory and inhibitory postsynaptic potentials, and the discharge of both excitatory and inhibitory neurons (the 'up' state), interdigitated with periods of hyperpolarization and quiescence (the 'down' state)[2–6]. The propagation and synchronization of this slow oscillation depends at least in part on corticocortical connections, and is proposed to be generated by recurrent excitation among large networks of cortical neurons, interrupted by periods of 'disfacilitation' in which the recurrent activity fails[5,6].

Although it was once thought that the generation of rhythmic activities in the electroencephalogram were due to the interaction of very large networks of neurons and therefore could only be studied *in vivo*, we have shown that at least one network oscillation, spindle waves, can be maintained in small networks of neurons *in vitro*[10]. Here we demonstrate generation of the slow rhythm in neocortical slices and show that this activity is generated through re-entrant excitation interspersed with failure of network activity.

Results

Intracellular recordings from primary visual cortical neurons in halothane-anesthetized cats revealed the rhythmic re-occurrence of depolarized and hyperpolarized membrane potentials[2–7] at a periodicity of once every 3.44 ± 1.37 seconds (n = 9; Fig. 1a–c). The depolarized phase appeared as a barrage of postsynaptic potentials that could reach action potential threshold and lasted an average of 1.08 ± 0.38 seconds (n = 9; Fig. 1a and b). The membrane potential during the slow oscillation exhibited a bimodal distribution with peaks at –71 ± 3.6 mV and –59.4 ± 4.9 mV, representing the up and down states[6–8].

Intracellular and extracellular recordings from ferret visual and prefrontal cortical slices maintained *in vitro* in 'traditional' slice bathing medium (2 mM Ca^{2+}, 2 mM Mg^{2+} and 2.5 mM K^{+}) did not reveal spontaneous rhythmic activities. However, changing the bath solution to more closely mimic the ionic composition of brain interstitial fluid *in situ*[12,13] (1.0 or 1.2 mM Ca^{2+}, 1 mM Mg^{2+} and 3.5 mM K^{+}) caused the appearance of spontaneous rhythmic oscillations that were nearly identical to those occurring *in vivo* (Fig. 1d–f; n = 87 visual cortical slices ; n = 5 prefrontal cortical slices). Once the slow oscillation developed, it was stable for the life of the slice (up to 12 h). It appeared as a depolarized state associated with action potential activity at 2–10 Hz (in regular spiking neurons), followed by a hyperpolarized state, recurring with a periodicity of once every 3.44 ± 1.76 seconds (n = 24; Fig. 1d–f). The membrane potentials again exhibited a bimodal distribution, with peaks at –68.7 ± 3.8 mV and –61.2 ± 4.8mV (n = 11). The depolarized state lasted for an average of 0.72 ± 0.43 seconds (n = 25 cells) and occurred in regular spiking (n = 13), intrinsically bursting (n = 11) and chattering (n = 20) pyramidal neurons, as well as fast-spiking local interneurons (n = 6) in phase with extracellularly recorded multi-unit activity (Figs. 1d and 6c; as also revealed with cross-correlograms; Methods).

Propagation of the slow oscillation

Extracellular multiple-unit recording with arrays of 8 microelectrodes (with inter-electrode spacing of approximately 0.25 or 0.5 mm; Fig. 2a) revealed that the slow oscillation was most robust and occurred first in or near layer 5, followed after a short delay by activity in deeper layers (layer 6), and finally after an addition-

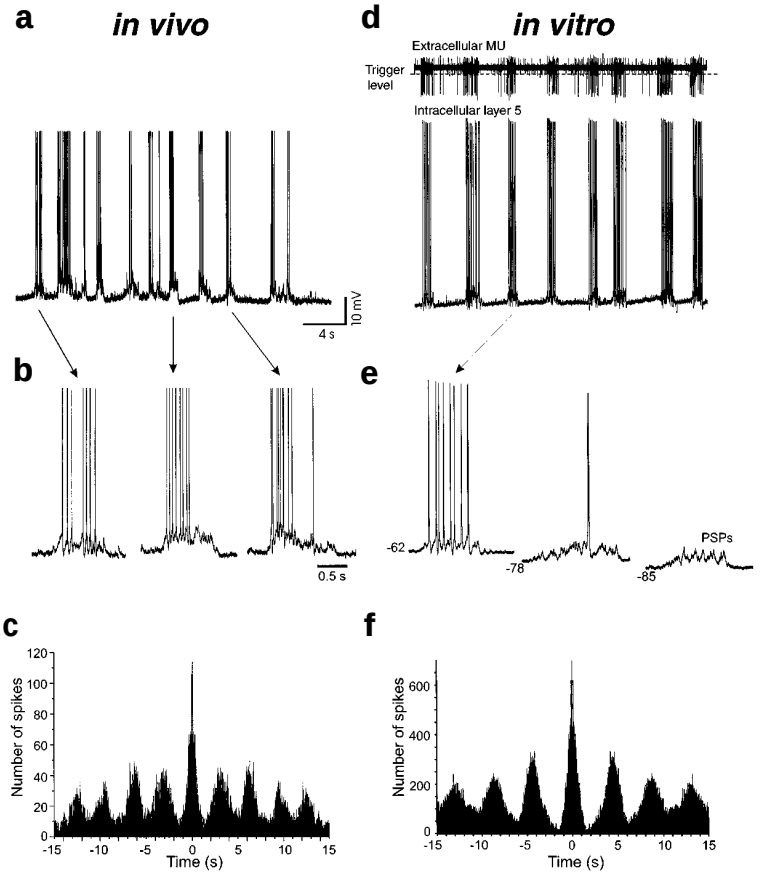

Fig. 1. Generation of the slow oscillation *in vivo* and *in vitro*. (**a**) Intracellular recording in the primary visual cortex of a halothane-anesthetized cat reveals a rhythmic sequence of depolarized and hyperpolarized membrane potentials. (**b**) Expansion of three of the depolarizing sequences for clarity. (**c**) Autocorrelogram of the intracellular recording reveals a marked periodicity of about one cycle per three seconds. (**d**) Simultaneous intracellular and extracellular recordings of the slow oscillation in ferret visual cortical slices maintained *in vitro*. Note the marked synchrony between the two recordings. The intracellular recording is from a layer 5 intrinsically bursting neuron. The trigger level for the window discriminator of the extracellular multi-unit recording is indicated. (**e**) The depolarized state at three different membrane potentials. (**f**) Autocorrelogram of the intracellular recording in (**d**) shows a marked periodicity of approximately once per 4 seconds.

al delay by activity in layers 2/3 (Fig. 2c and d). The timing and intensity of discharges in the different layers were compared using two methods. First, cross-correlations were calculated between the multiple-unit activity recorded from each of the electrodes. Cross-correlations are most sensitive to the relative timing of the peak of action potential activity between the two recording sites, and less sensitive to the onset of activity. Cross-correlations between multi-unit recordings in layer 5 and those in layer 6 revealed an average difference of 10.5 ± 10.2 ms (n = 6 slices; $p < 0.05$), whereas cross-correlations between layer 5 and activity in layers 2/3 revealed an average delay of 28.0 ± 16.3 ms (n = 6 slices; $p < 0.01$; data not shown). To better examine and illustrate the timing of activity in the different layers, we calculated the average activity in each recording site (peri-event histogram) relative to the peak of activity that occurred in the layer 5 recording site during each up state of the slow oscillation. Neurons in layer 5 initiated an increase in neuronal discharge 32 ± 24 ms (n = 8; $p < 0.01$) before activity in layer 6 and 127 ± 60 ms (n = 8; $p < 0.01$) before increases in activity in layers 2/3 (Fig. 2d). In addition, the peak of activity in layer 5 was always larger than in any other layer, and activity in this layer persisted for a longer period than in other layers (Fig. 2d).

Spontaneous action potential activity between bursts of the slow oscillation was prominent in infragranular layers, particulary in or near layer 5 (Fig. 2b and d). This spontaneous activity typically decreased immediately following the up phase of the slow oscillation (Fig. 2d) and recovered over the next second or more. Spontaneous activity during the down state was relatively absent in layers 2/3 (Fig. 2b and d).

Placement of a horizontal array of electrodes along layers 5 and 6 demonstrated that the slow oscillation propagated along these layers (Fig. 3). Calculating the rate of propagation of the slow oscillation according to the shift in the cross-correlogram yielded a value of 10.9 ± 3.0 mm/s (n = 11 slices; Fig. 3d). Similarly, calculating the average multi-unit activity generated at each recording site relative to the peak of activity (during the up state) in the first electrode of the array also revealed a progressive shift in the peak activity to longer and longer delays with increasing distances between recording electrodes (Fig. 3e). The cumulative histograms plotted in this manner, however, revealed considerable spread in time, presumably owing to variations at the timing of action potential activity at the various electrodes relative to the peak of activity in the reference electrode (Fig. 3e).

The horizontal propagation of the slow oscillation could occur in either direction, although a dominant direction of propagation was often observed in each slice (Fig. 4a). The slow oscillation could also start near one of the middle electrodes of the array (either spontaneously or in response to a local application of glutamate) and propagate in both directions away from this initiation point (Fig. 4). In one slice, the propagation of the slow oscillation was typically in the direction of electrodes 1 to 8, which were placed horizontally in layers 5/6 (Fig. 4a and b). Occasional 'backward' propagation from electrodes 8 to 1 occurred spontaneously (Fig. 4a). The activation of the slow oscillation at electrode 8 with local picodrop application of glutamate (1 mM in the micropipette) once every six seconds resulted in the immediate transition to backward propagation of the slow oscillation (Fig. 4a and b), although forward propagation still occurred spontaneously on occasion (Fig. 4a). Application of glutamate to the slice near the middle electrode (electrode 4) resulted in the initiation of the slow oscillation at this site and propagation in both directions (Fig. 4b).

To quantify these effects, we calculated cross-correlograms between electrodes at both ends of the array (that is, electrodes 1 and 8) for spontaneous and glutamate-induced local activation of the slow oscillation. The cross-correlograms for spontaneously occurring slow oscillations revealed two peaks corresponding to forward and backward propagation, as well as side peaks illustrating the periodicity of the slow oscillation (Fig. 4c; the peak to the left of zero seconds represents propagation from electrodes 1 to 8, whereas the small peak to the right of zero represents the occasional propagation in the reverse direction). In contrast to

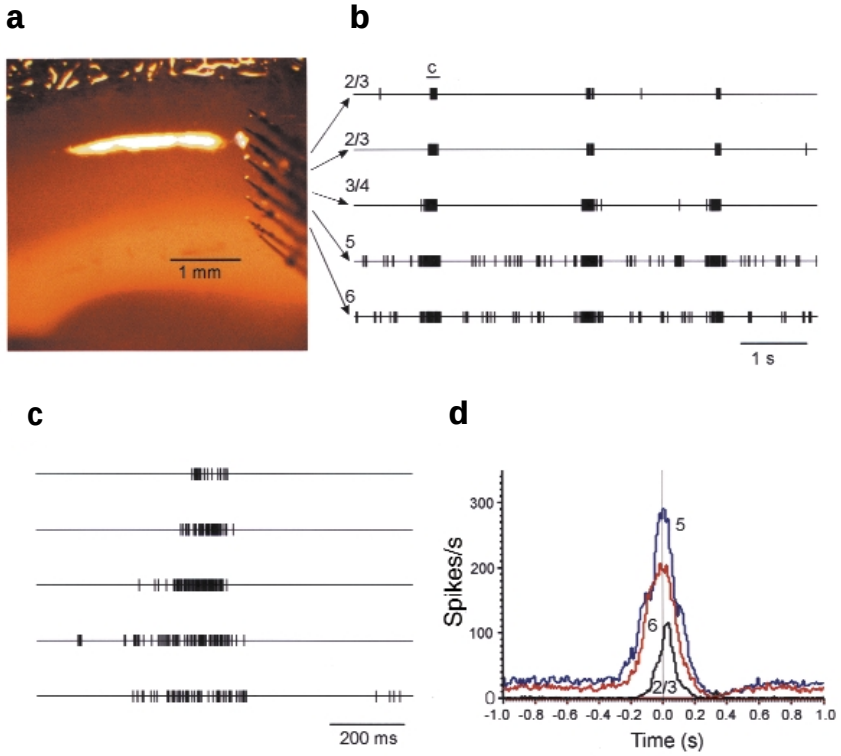

Fig. 2. The slow oscillation is generated first around layer 5 and propagates vertically. (**a**) The extracellular recording microelectrode array (0.25 mm interelectrode spacing) placed vertically in the cortical slice. (**b**) Simultaneous extracellular multiple-unit recording from layers 2/3 to 6 reveal the slow oscillation to initiate around layer 5, followed, on average, by activity in layers 6 and 2/3. The burst of activity indicated is expanded in (**c**). The third electrode was at the border between layers 3 and 4, whereas the fourth electrode was at the top of layer 5. Electrodes 6–8 did not yield useful multi-unit recordings. Each tic mark represents a detected action potential in the multi-unit recording. (**d**) Unit histograms aligned to the peak of activity in layer 5 for each of the up states of the slow oscillation reveals that layers 5 and 6 generate spontaneous activity before the onset of the up state, but that this activity decreases following the up state. The up state begins slightly earlier in layer 5 than layer 6 and is more intense.

these results, calculation of the cross-correlograms between electrodes 1 and 8 during the initiation of the slow oscillation with the local application of glutamate once every six seconds at electrode 8 revealed not only that the dominant direction of propagation of the slow oscillation was reversed, but also that the oscillation was more regular owing to its initiation by the glutamate applications (Fig. 4c). These results indicate that the initiation of the slow oscillation may take place anywhere within the cortical slice, and presumably occurs spontaneously at the site with the shortest refractory period. The slow oscillation seems to propagate horizontally as a column of activity that appears earliest in or near layer 5 but then occurs shortly thereafter in the deeper and more superficial layers.

The slow oscillation is distinct from epileptiform activity

Epileptiform network activity in neocortical slices is generated and propagated in response to block of $GABA_A$ receptors or removal of Mg^{2+} from the bath[14–17]. Similarly, blocking $GABA_A$ receptors with picrotoxin (25 μM, bath) or bicuculline (20 μM, bath) slowly transformed the slow oscillation into epileptiform activity, such that the up period was initially changed from a continuous barrage of activity to a reverberation of 2–4 brief (0.1–0.2 s) bursts of activity at 2–5 Hz, and the down period was relatively unaltered. However, following increasing block of $GABA_A$ receptors, periods of epileptiform activity appeared suddenly; they were characterized by intense bursts of tonic activity of 0.3–5 seconds in duration, which had the highest frequency of discharge within the first 100 ms (n = 14 of 36 recording sites in 5 slices) and propagated at 89.8 ± 33.1 mm/s. This tonic activity was followed, in other recording sites (n = 22 of 36), by rhythmic, intense bursts of action potentials at an average interburst frequency of 1.5 ± 0.3 Hz (n = 13) that lasted for approximately 1.5 to 20 seconds (data not shown).

Changing bath Mg^{2+} concentration to 0 mM (n = 3 slices) also resulted in epileptiform activity distinct from the slow oscillation. Washing Mg^{2+} out of the bathing medium resulted in a gradual increase in frequency of the slow oscillation (up to 1.2–1.7 Hz), followed by a sudden transition to the generation of prolonged epileptiform bursts of activity[15,16]. These bursts of activity were associated in the multiple-unit recordings with a rapid increase in firing that peaked within 100 ms and propagated at 17.6 ± 2.9 mm/s (n = 8 events), followed by a steady decline over the next 8–10 seconds. This tonic activity transformed into rhythmic bursts of synchronized discharge at 1.25 to 2.5 Hz for an additional 7–16 seconds. These events recurred approximately once every 59–79 seconds. The epileptiform events generated in picrotoxin, bicuculline or low Mg^{2+} are markedly distinct from those generated by the slow oscillation: they show a stronger discharge of prolonged, tonic neuronal activity and rhythmic discharges of a higher frequency, and they propagate at a significantly higher rate and recur only about once per minute or longer.

Slow oscillation propagates through all layers

To identify the path of propagation of the spontaneous slow oscillation, we made various knife cuts during preparation of the cortical slices. When we recorded simultaneously on either side of vertical knife cuts (perpendicular to the pia) through layers 2/3, horizontal propagation was not prevented (as revealed by cross-correlograms; Methods; n = 10 slices). Similarly, knife cuts extending through the white matter and layers 5/6, but leaving intact layers 1–3 and sometimes portions of layer 4, also did not prevent the propagation of the slow oscillation, as revealed by simultaneous recordings in layers 5/6 on both sides of the cut and the calculation of cross-correlograms (n = 6 slices; Fig. 5). However, the block of non-NMDA glutamatergic ionotropic receptors with the local application of CNQX (0.2–0.5 mM in micropipette) in layer 2/3 (in slices in which the deep layers were cut) abolished the horizontal propagation of the slow oscillation (n = 4; Fig. 5). Similarly, local application of CNQX to intact (uncut) slices also blocked the horizontal propagation of the slow oscillation (without blocking the slow oscillation on either side of the local application), but only if it was applied throughout layers 2–6 and covered a horizontal extent of the slice of

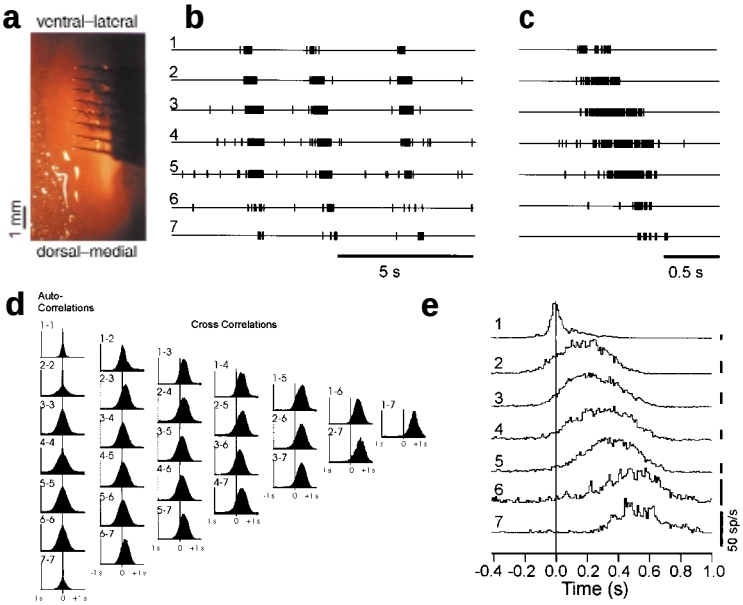

Fig. 3. The slow oscillation propagates horizontally. (**a**) The multi-electrode array (0.5 mm interelectrode spacing) placed on a cortical slice. (**b**) Extracellular multiple-unit recording electrodes placed in the deep cortical layers show that the slow oscillation propagates horizontally at about 6 mm/s (expanded in **c**). (**d**) Auto- and cross-correlograms illustrating the synchronized nature of the slow oscillation and the progressive propagation of this activity. (**e**) Unit histograms aligned to the peak of activity in electrode 1 show that the peak of activity in each electrode occurs progressively later in time with increasing distance from the reference electrode.

approximately 1–2 mm (n = 3; data not shown).

Bath application of the NMDA receptor antagonist APV (50–100 μM) blocked the slow oscillation (n = 4 of 7 slices) or greatly reduced the intensity of discharge (n = 3 of 7) as recorded in layers 5/6. In contrast, bath application of the non-NMDA glutamate receptor antagonist CNQX (10 μM; n = 2 slices) resulted in a rapid block of the slow oscillation throughout all layers, but did not block all spontaneous action potential activity in the infragranular layers. Washout of CNQX or APV reversed all these effects.

To examine if the superficial or deep cortical layers may independently generate the slow oscillation, we prepared slices that were cut horizontally (parallel to the pia) through the middle of the cortex, thereby completely separating the supragranular and infragranular layers. Slices containing layers 5/6 reliably generated the slow oscillation (n = 11 of 12 slices), whereas slices containing the superficial, but not the deep, layers either generated a weak slow oscillation (n = 5 of 12 slices) or none at all (n = 7 of 12; as shown by multiple-unit recordings). Slices that contained layers 1–6 and were less than 0.5–1.0 mm wide (0.4 mm thick) also generated the slow oscillation, suggesting that this rhythm may occur within a single cortical column (n = 4).

Synaptic activity underlying slow oscillations

Intracellular recordings from all four electrophysiological cell types revealed the slow oscillation to be associated with a depolarized up state consisting of barrages of both excitatory and inhibitory postsynaptic potentials (Fig. 6a; QX 314 in the electrode; n = 9). Blocking the IPSPs with bicuculline (local; 200–300 μM in micropipette; n = 3) strongly increased the amplitude of the depolarized state (Fig. 6b). Similarly, physiologically identified GABAergic fast-spiking neurons[18] (n = 6) discharged only during the up state of the slow oscillation, in synchrony with multi-unit activity in neighboring neurons (Fig. 6c and d).

Persistent firing may result from either synaptic barrages or intrinsic membrane properties[19–21]. Hyperpolarization or depolarization of cortical neurons by 10 to 20 mV with the intracellular injection of direct current did not change either the duration of the depolarized state (0.60 ± 0.12 s depolarized; 0.68 ± 0.23 s hyperpolarized) or the slow oscillation frequency in the recorded neuron (0.5 ± 0.15 Hz depolarized; 0.54 ± 0.13 Hz hyperpolarized; n = 5 cells). These results indicate that the slow oscillation is generated as a network event and not intrinsically in the neuron recorded.

Refractory period of slow oscillations

The cellular basis of the down state of the slow oscillation was investigated with both extracellular and intracellular recordings. Local activation of small regions of cerebral cortex with glutamate (0.5 mM) application resulted in the initiation and propagation of the slow oscillation (Fig. 4). That the glutamate was activating the slow oscillation and not merely activating a barrage of action potentials in the extracellular multiple-unit recordings is shown by the similarity of the action potential barrage in response to glutamate to that occurring spontaneously during the slow oscillation (for example, Figs. 4b and 7a), as well as the propagation of the slow oscillation away from the recording site (Fig. 4).

Repeated application of glutamate at various intervals revealed a relative refractory period, requiring 3–6 seconds before the application of glutamate resulted in a full discharge of extracellularly recorded multiple-unit activity (Fig. 7a and b; n = 5 slices). Spontaneously occurring slow oscillations could occur and interact with those triggered by local application of glutamate, if the periodicity of glutamate application was substantially different from the endogenous periodicity of the slow oscillation. If glutamate activated a local burst of action potentials just before (1–2 s) the occurrence of a spontaneous slow oscillation, then the site activated by glutamate discharged only weakly in response to the slow oscillation. Similarly, if the up state of the slow oscillation occurred spontaneously just before the application of glutamate, then the evoked response to this agonist was markedly diminished (data not shown). These results indicate that the discharge of action potentials associated with the up state of the slow oscillation is followed by a relative refractory period of several seconds.

Intracellular recordings from putative pyramidal or spiny stellate cells during the slow oscillation showed that the depolarizing phase of the oscillation was followed by a slow afterhyperpolarization (AHP; n = 24), the duration of which matched the duration of the down state or refractory period (Fig. 7c and d). This AHP was associated with an increase in apparent input conductance of 12.2 ± 4.6 nS (n = 10) at the peak, as determined by the response to intracellular injection of hyperpolarizing and depolarizing current pulses of 0.1 nA and following compensation for changes in the membrane potential. The slow AHP exhibited a reversal potential of –87.3 ± 11.0 mV (n = 9), as determined by the calculation of current–voltage plots from current pulses injected at the peak of the AHP in comparison to those occurring just before onset of the up state. This reversal potential suggests that the AHP is mediated by an

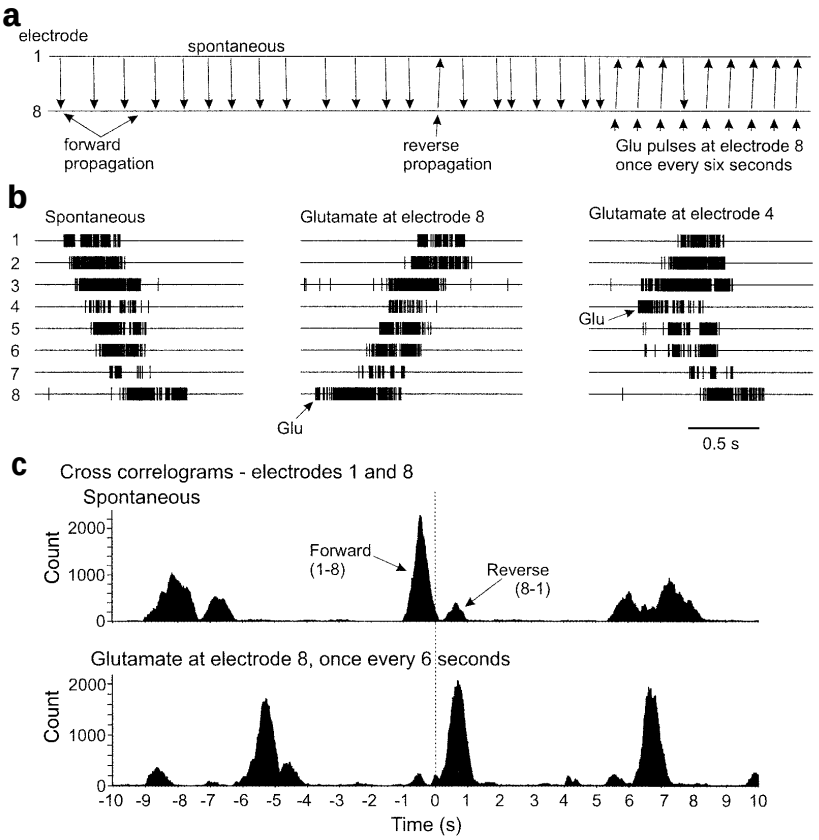

Fig. 4. Local application of glutamate can initiate the slow oscillation. (**a**) Schematic of the direction of propagation of the slow oscillation in a portion of one experiment. The oscillation typically traveled from electrode 1 to 8, although occasional reverse propagation occurred spontaneously. Local picodrop application of glutamate (1 mM in micropipette) near electrode 8 resulted in the initiation of the slow oscillation at this electrode and reverse propagation to electrode 1. (**b**) Single examples of spontaneous forward propagation and reverse propagation initiated by applying glutamate at electrode 8. Application of glutamate at electrode 4 initiated the slow oscillation at this electrode, which then propagated in a 'V-like' fashion in both directions. (**c**) Cross-correlograms between activity in electrodes 1 and 8 during spontaneous generation of the slow oscillation and during activation of this network activity with local application of glutamate at electrode 8 once every 6 seconds. Note that during spontaneous generation, the cross-correlogram reveals electrode 1 consistently leading electrode 8, a pattern that is reversed when the slow oscillation is initiated at electrode 8 with glutamate application. Note also that the slow oscillation is more regular when initiated once every six seconds by local glutamate application. The small side peaks in the cross-correlograms result from the occasional reverse propagation of the slow oscillation.

increase in K^+ conductance. Mimicking the discharge of cortical neurons during the up state of the slow oscillation through the intracellular injection of depolarizing current pulses (5–6 pulses of 50 ms each; $n = 5$) resulted in a slow AHP similar to that occurring during the spontaneous slow oscillation. This result indicates that the slow AHP is generated through intrinsic mechanisms.

The slow AHP during the refractory period of the spontaneous slow oscillation was associated with a marked decrease in response of cortical pyramidal cells to the intracellular injection of depolarizing current pulses (Fig. 7d; $n = 10$). The slow AHP following bursts of action potential activity was not prevented by blocking $GABA_A$ receptors with bicuculline methiodide (200 μM; $n = 3$; Fig. 6b) or picrotoxin (25 μM; $n = 4$) or blocking $GABA_B$ receptors with CGP35348 (200 μM in bath; $n = 4$), indicating that these AHPs are not generated through the activation of GABA receptors.

Discussion

The cerebral cortex can spontaneously generate a slow rhythm (0.1–0.5 Hz) during anesthesia and slow-wave sleep characterized by recurring periods of activity that last for approximately 0.5–1.5 seconds[2–8]. Here we have demonstrated that this slow oscillation can also occur in cortical slices maintained *in vitro*, as long as the ionic concentrations of the bathing medium are close to those found *in situ*[12,13]. Together, these *in vivo*[2–7] and *in vitro* intracellular recordings reveal that the active period of the slow oscillation (the 'up' state) is associated with a depolarization of all cell types, mediated by a mixture of excitatory and inhibitory postsynaptic potentials. The period between active periods (the 'down' state) is associated with the withdrawal of synaptic barrages as well as the generation of an afterhyperpolarization in pyramidal or spiny stellate neurons[5,6]. These results suggest that the slow oscillation of the neocortex is generated through a recurrent network of excitatory connections that, through re-entrant loops of activity, generate a self-sustained period of depolarization that can be initiated by layer 5 pyramidal neurons, but propagates to deeper and more superficial layers. The occurrence of spontaneous activity in infragranular neurons between up states suggests that these cells are on average more depolarized, either through intrinsic or synaptic mechanisms, than supragranular cells. This relative depolarization of infragranular neurons may allow them to be more sensitive to the spread of neuronal activity in the cortical network, thereby discharging first, on average, in response to the arrival of the up state of the slow oscillation. The amplitude of the depolarization, the so-called 'up' state, is controlled by the activation of GABAergic inhibitory neurons and perhaps by intrinsic K^+ conductances. This period of activity can persist for up to a couple of seconds, even though the discharge rate of individual neurons is typically low (< 10 Hz). In the *in vitro* slice preparation, the slow oscillation then propagates horizontally at a rate (11 mm/s) that is considerably slower than axon conduction velocities[22]. We hypothesize that the rate of propagation of this activity is determined in large part by the time required to bring each successive neuron to spike threshold. Recordings of the slow oscillation *in vivo* reveal that it occurs throughout the cerebral cortex and may propagate at a considerably higher rate (approximately 100 mm/s)[23], presumably owing to extensive corticocortical connections.

What generates the slow periodicity of the slow oscillation? We propose that the failure of the network to maintain the self-activated state occurs when the buildup of outward conductances, such as Ca^{2+} and Na^+-activated K^+ currents[25,26], overcomes the

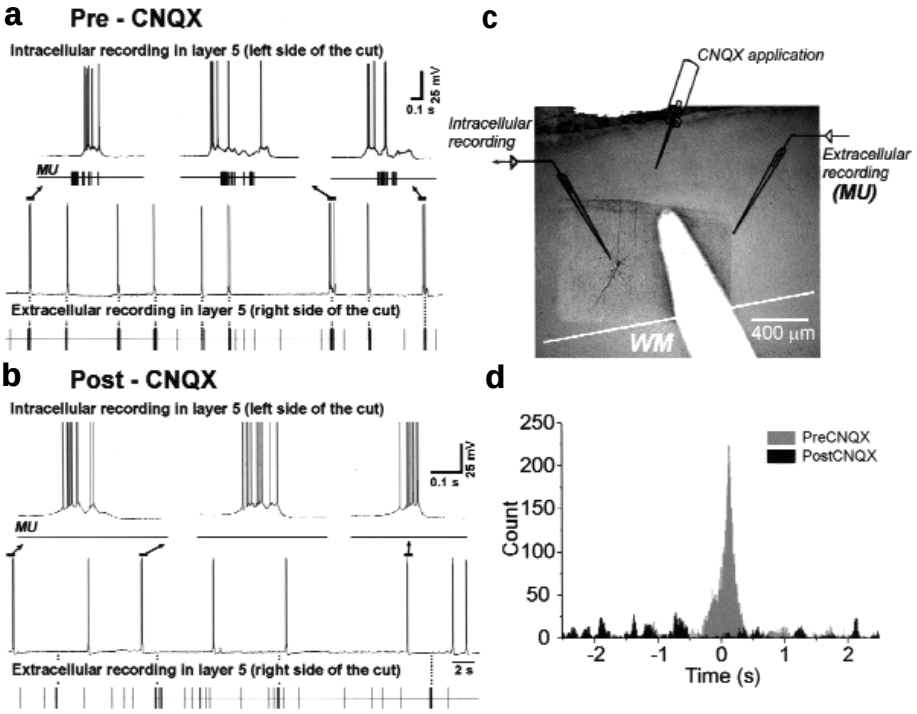

Fig. 5. The slow oscillation can propagate through supragranular layers and depends on excitatory transmission. (**a**) Simultaneous intracellular and extracellular recording of the slow oscillation on either side of a knife cut that extends through the white matter and layers 4–6. Note the synchrony in activity between the two recordings (MU, multi-unit recording). (**b**) Application of the non-NMDA glutamate receptor antagonist CNQX to layer 2–3 above the knife cut results in a loss of synchrony between the slow oscillations recorded on the two sides of the knife cut, whereas independent oscillations are generated on both sides. (**c**) Slice containing the intracellularly biocytin-labeled inverted pyramidal cell in layer 5 (left), showing the position of the extracellular recording electrode on the right. (**d**) Cross-correlograms show synchrony before application of CNQX, and its loss afterward.

positive feedback inherent in local cortical circuits[27,28]. The network then rapidly fails, and the persistence of the outward currents generates a prolonged hyperpolarization (the down state)[5,6]. Because the activity associated with the up state ceases or decreases dramatically during the down state, the slow afterhyperpolarization slowly decreases in amplitude, allowing the network to again generate another up state. According to this hypothesis, the periodicity of the slow oscillation is determined largely by the balance between the recurrent excitation and inhibition inherent in cortical networks, and the time course of the outward currents generating the slow afterhyperpolarization. An alternative hypothesis is that the duration of the up state is limited by the readily releasable pool of excitatory neurotransmitter at intracortical synapses[29]. However, this hypothesis is not consistent with the finding that β-adrenergic agents, which block slow AHPs in cortical neurons[30], cause replacement of the slow oscillation with a continuous 2–3 Hz rhythm (J.B. Brumberg, M.V.S.-V. and D.A.M., *Soc. Neurosci. Abstr.* 26, 2000), or with the finding that bath application of picrotoxin or nominal Mg^{2+} results in intense discharges that far outlast the duration of the up state of the slow oscillation.

Functional consequences of persistent activity

In vivo, the up and down states of spontaneous cortical network activity are associated with marked increases and decreases, respectively, in the responses to sensory stimuli[5,31]. These spontaneous patterns of activity are highly state dependent. Repetitive stimulation of the ascending activating systems in the brainstem abolish the slow oscillation in the EEG, cause cortical neurons to maintain a persistently depolarized state[32], and dramatically increase the amplitude of sensory evoked cortical responses[33]. These results suggest that local or global regions of the cerebral cortex are capable of rapidly swinging between excitable and less excitable states either in response to activity intrinsic to the cerebral cortex or in response to exogenous influences (for example, a volley of activity in excitatory afferent pathways or the release of a neuromodulatory agent). Rapid changes in the excitability of cortical neurons have not only been associated with the generation of EEG sleep rhythms, but have also been found in awake behaving animals during selective attention[36,37] and short-term memory tasks[38]. Indeed, reverberating loops of neuronal activity within cortical circuits are often proposed as a possible mechanism for short-term storage of information[21,39,40]. More specifically, computational models suggest that reverberating cortical networks may generate the persistent activity in prefrontal cortical neurons associated with performance of delayed-response memory tasks in primates[21]. Our results provide direct evidence for the ability of local cortical circuits in the prefrontal cortex to generate periods of sustained activity, even without subcortical and long-range inputs. Questions remain as to the mechanisms by which local neuronal networks stay relatively independent of one another during the up state, how the networks may avoid disruptions by the occurrence of 'distractors', and whether or not single neurons can participate in multiple 'cliques' of neurons either sequentially or simultaneously.

Is there a role for sustained or recurrent activity in primary and secondary visual cortical areas? The generation of rhythmic periods of persistent activity is a property of many, if not all, areas of the cerebral cortex[2–6]. Although primary visual areas generate slow oscillations during sleep, the activity of these neurons is thought to be highly dependent on visual stimuli in awake, behaving animals. However, significant spontaneous activity does occur in the primary visual cortices of awake, attentive animals without visual stimulation (even in the dark), although this activity is restricted to the cortical layers that receive direct thalamic input, which is also spontaneously active[41]. At least in anesthetized animals, spontaneous activity in single visual cortical neurons is associated with a pattern of cortical activation similar to that occurring when the cell is stimulated by a preferred visual stimulus[24]. This result implies that spontaneous activity in cortical networks is far from random, and may represent a bias state of the local network. Finally, the operation of recurrent networks in primary visual cortex may be important in the generation of receptive field properties in at least some neuronal subtypes[27,28] (but see refs. 42, 43).

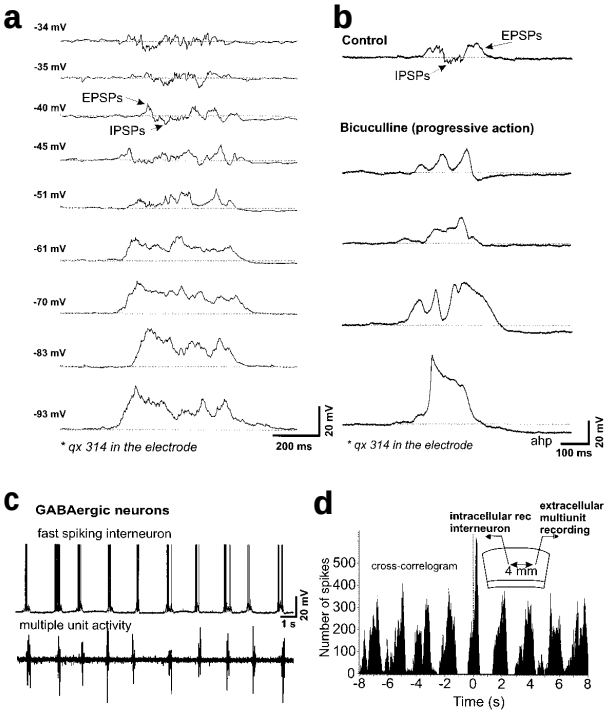

Fig. 6. The postsynaptic potentials underlying the depolarized state consist of both excitatory and inhibitory events. (**a**) Intracellular recording with an electrode containing the Na^+ channel blocker QX-314 (50 mM) to block the generation of action potentials in this cell. Moving the cell to different membrane potentials with the intracellular injection of current reveals the postsynaptic potential barrage to consist of both depolarizing (excitatory) and hyperpolarizing (inhibitory) postsynaptic potentials. (**b**) The local application of the $GABA_A$ receptor antagonist bicuculline (0.5 mM in micropipette) to another cell results in a block of the IPSPs and the transformation of the depolarizing event into an epileptiform paroxysmal depolarization shift (PDS)[19]. (**c**, **d**) Simultaneous intracellular recording from a fast-spiking GABAergic inhibitory cell and multiple-unit activity show that the GABAergic neuron discharges during the up state of the slow oscillation and not during the down state (**c**). Cross-correlation of firing in the fast-spiking neuron and the extracellular multi-unit activity shows a positive correlation with a peak at 0.25 seconds and a marked periodicity of once every 1.8 seconds (**d**).

We suggest that a basic operation of cortical networks is the generation of self-maintained depolarized states that are tightly regulated through the interaction with local GABAergic neurons and intrinsic membrane conductances. Sleep represents a state when the network spontaneously 'sputters', or starts and stops, owing to reduced excitability of the cortical neurons and network[2–7]. In contrast, epileptiform activity arises when cortical networks become over-excitable and control of the re-entrant excitation is lost[11,14]. Finally, the ability of cortical networks to generate persistent and recurring activities even without ongoing subcortical inputs suggests that this process may underlie perceptual influences on sensory information processing, briefly encode short-term memories, and generate dreams during slow-wave and rapid eye movement sleep and hallucinations when left unconstrained in the awake brain.

METHODS

Intracellular recordings *in vivo* were obtained in the primary visual cortex of halothane-anesthetized cats as described[44]. *In vitro* experiments were done on 0.4 mm thick slices mainly from the lateral portions of the ferret occipital cortex, including primary and secondary (areas 17, 18 and 19) visual cortical areas or prefrontal cortex. The slices were maintained in an interface-style recording chamber at 35° C as described[25]. Slices were formed on a DSK microslicer (Ted Pella, Redding, California) in a slice solution in which the NaCl was substituted with sucrose.

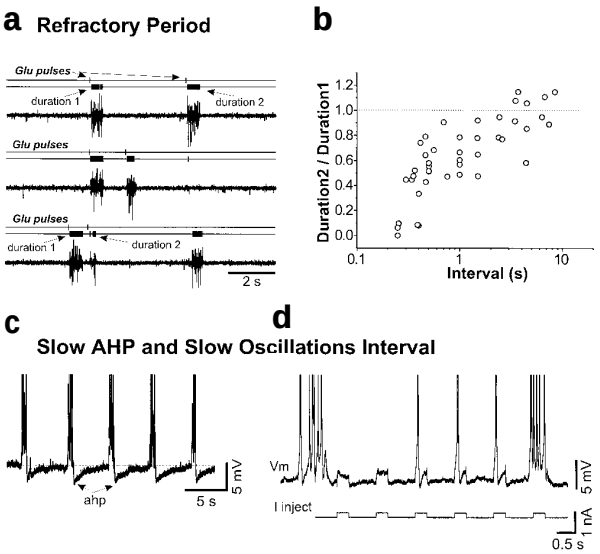

Following transfer to the recording chamber, the slices were incubated in 'traditional' slice solution containing 124 mM NaCl, 2.5 mM KCl, 2 mM $MgSO_4$, 1.25 mM $NaHPO_4$, 2 mM $CaCl_2$, 26 mM $NaHCO_3$ and 10 mM dextrose, aerated with 95% O_2, 5% CO_2 to a final pH of 7.4. After approximately 1 hour, the slice solution was modified to contain 1 mM $MgCl_2$, 1 or 1.2 mM $CaCl_2$ and 3.5 mM KCl. In some experiments, the slices were carefully cut (before placement in the interface recording chamber) as described in the results section. Following each experiment, the slices were fixed in paraformaldehyde, sectioned at 60–75 μm, stained with cresyl violet, and examined under the microscope to confirm the extent of the knife cuts and the laminar location of each recording site. Extracellular multiple unit recordings were obtained with either single electrodes or electrode arrays (Frederick Haer, Bowdoinham, Maine). Activity in vertical arrays of electrodes from layers 2 through 6 was recorded in area 18 of the ferret visual cortex, which has a much smaller layer 4 than area 17. Horizontal propagation of activity was measured with electrode arrays placed in infragranular layers in both areas 17 and 18. Intracellular recordings were done with beveled sharp microelectrodes containing 2 M potassium acetate and, in some cells, 2% biocytin for identification of neuronal morphology. Drugs were either applied in the bath or through the delivery of a brief pulse of nitrogen to a drug-containing micropipette (volumes of 10–20 pl), as indicated in the text. Signals were digitized, acquired and analyzed with a 1401 interface and Spike2 software (CED, Cambridge, UK).

Fig. 7. The slow oscillation has a refractory period associated with hyperpolarization and decreased excitability. (**a**, **b**) Local application of brief pulses of glutamate (0.5 mM in micropipette) was used to initiate the slow oscillation. Glutamate-induced slow oscillations were indistinguishable from spontaneously occurring ones (for example, see lower set of traces in **a**). Decreasing the interval between the generation of either spontaneous or glutamate-activated burst of action potentials and another one initiated by glutamate application (**a**) resulted in a marked decrease in the relative duration of the second, activated response (**b**). This refractory period had a duration of approximately 3–5 seconds. (**c**, **d**) The slow oscillation is associated with a slow afterhyperpolarization (**c**; AHP) that results in a marked decrease in the response of this layer 2/3 cell to intracellular injection of a depolarizing current pulse (**d**).

The propagation, synchrony, duration and frequency of the oscillations were analyzed with auto- or cross-correlograms. The rate of propagation was calculated with the offset of the central peak in cross-correlograms between electrodes at a known distance apart. For multiple-site recordings (for example, Fig. 3), the propagation velocity was averaged over all electrodes. The temporal relationship between the neuronal activities at varying recording sites was examined with cross-correlograms. All such cross-correlograms (except following the application of CNQX; Results) showed prominent peaks, depending on the distance between the recording sites and the rate of propagation of the activity under study (Figs. 3, 5 and 6). The duration of the up state of the slow oscillation was measured as half the width of the central peak in autocorrelograms, whereas the frequency was measured as the average interpeak interval (for example, Fig. 1c and f). Duration and frequency of the oscillations at different membrane potentials (both supra- and subthreshold) were calculated from autocorrelograms of the membrane potential values. The bimodal distribution of the membrane potential was calculated from histograms of membrane potential values (100–200 s at 5 KHz). The peak value was obtained by Gaussian fitting. Propagation of the slow oscillation across vertical knife cuts was also measured with cross-correlograms between recording sites on either side of the cuts (for example, Fig. 5d). Comparator thresholds in each recording were all set to the same value (20–30 microvolts; approximately 2 × background noise levels; Fig. 1d) to prevent bias in the site of initiation of the slow oscillation. The onset of the slow oscillation in peri-event histograms was measured as the point in which the base of the peak response deviated from the average firing rate.

Acknowledgements

We thank L. G. Nowak for participation in critical portions of these experiments. We thank L. Nowak, A. Luthi, J. Brumberg, H. Blumenfeld and R. Gallego for comments on the manuscript. This work was supported by the NIH and the McKnight Foundation. For movies and additional information see www.mccormicklab.org.

Received 13 June; accepted 4 August 2000

1. Steriade, M., McCormick, D. A. & Sejnowski, T. Thalamocortical oscillations in the sleeping and aroused brain. *Science* 262, 679–685 (1993).
2. Steriade, M., Nunez, A. & Amzica, F. A novel slow (< 1 Hz) oscillation of neocortical neurons *in vivo*: depolarizing and hyperpolarizing components. *J. Neurosci.* 13, 3252–3265 (1993).
3. Steriade, M., Contreras, D., Curro Dossi, R. & Nunez, A. The slow (< 1 Hz) oscillation in reticular thalamic and thalamocortical neurons: scenario of sleep rhythm generation in interacting thalamic and neocortical networks. *J. Neurosci.* 13, 3266–3283 (1993).
4. Steriade, M., Nunez, A. & Amzica, F. Intracellular analysis of relations between the slow (< 1 Hz) neocortical oscillation and other sleep rhythms in the electroencephalogram. *J. Neurosci.* 13, 3266–3283 (1993).
5. Contreras, D., Timofeev, I. & Steriade, M. Mechanisms of long-lasting hyperpolarizations underlying slow sleep oscillations in cat corticothalamic networks. *J. Physiol. (Lond.)* 494, 251–264 (1996).
6. Metherate, R. & Ashe, J. H. Ionic flux contributions to neocortical slow waves and nucleus basalis-mediated activation: whole-cell recordings *in vivo*. *J. Neurosci.* 13, 5312–5323 (1993).
7. Lampl, I., Reichova, I. & Ferster, D. Synchronous membrane potential fluctuations in neurons of the cat visual cortex. *Neuron* 22, 361–374 (1999).
8. Stern, E. A., Kincaid, A. E. & Wilson, C. J. Spontaneous subthreshold membrane potential fluctuations and action potential variability of rat corticostriatal and striatal neurons *in vivo*. *J. Neurophysiol.* 77, 1697–1715 (1997).
9. Achermann, P. & Borbely, A. A. Low-frequency (< 1 Hz) oscillations in the human sleep electroencephalogram. *Neuroscience* 81, 213–222 (1997).
10. von Krosigk, M., Bal, T. & McCormick, D. A. Cellular mechanisms of a synchronized oscillation in the thalamus. *Science* 261, 361–364 (1993).
11. Steriade, M. & Contreras, D. Relations between cortical and thalamic cellular events during transition from sleep patterns to paroxysmal activity. *J. Neurosci.* 15, 623–642 (1995).
12. Yamaguchi, T. Cerebral extracellular potassium concentration change and cerebral impedance change in short-term ischemia in gerbil. *Bull. Tokyo Med. Dent. Univ.* 33, 1–8 (1986).
13. Zhang, E. T., Hansen, A. J., Wieloch, T. & Lauritzen, M. Influence of MK-801 on brain extracellular calcium and potassium activities in severe hypoglycemia. *J. Cereb. Blood Flow Metab.* 10, 136–139 (1990).
14. Connors, B. W. Initiation of synchronized neuronal bursting in neocortex. *Nature* 310, 685–687 (1984).
15. Telfeian, A. E. & Connors, B. W. Epileptiform propagation patterns mediated by NMDA and non-NMDA receptors in rat neocortex. *Epilepsia* 40, 1499–1506 (1999).
16. Avoli, M., Drapeau, C., Louvel, J., Olivier, A. & Villemure, J. G. Epileptiform activity induced by low extracellular magnesium in the human cortex maintained *in vitro*. *Ann. Neurol.* 30, 589–596 (1991).
17. Chagnac-Amitai, Y. & Connors, B. W. Horizontal spread of synchronized activity in neocortex and its control by GABA-mediated inhibition. *J. Neurophysiol.* 61, 747–758 (1989).
18. McCormick, D. A., Connors, B. W., Lighthall, J. W. & Prince, D. A. Comparative electrophysiology of pyramidal and sparsely spiny neurons of the neocortex. *J. Neurophysiol.* 54, 782–806 (1985).
19. Raman, I. M. & Bean, B. P. Ionic currents underlying spontaneous action potentials in isolated cerebellar Purkinje neurons. *J. Neurosci.* 19, 1663–1674 (1999).
20. Haj-Dahmane, S. & Andrade, R. Ionic mechanism of the slow afterdepolarization induced by muscarinic receptor activation in rat prefrontal cortex. *J. Neurophysiol.* 80, 1197–1210 (1998).
21. Wang, X.-J. Synaptic basis of cortical persistent activity: the importance of NMDA receptors to working memory. *J. Neurosci.* 19, 9587–9603 (1999).
22. Nowak, L. G. & Bullier, J. in *Cerebral Cortex: Extrastriate Cortex in Primates* Vol. 12 (eds. Rockland, K., Kaas, J. H. & Peters, A.) 205–241 (Plenum, New York 1997).
23. Amzica, F. & Steriade, M. Short- and long-range neuronal synchronization of the slow (< 1 Hz) cortical oscillation. *J. Neurophysiol.* 73, 20–38 (1995).
24. Tsodyks, M., Kenet, T., Grinvald, A. & Arieli, A. Linking spontaneous activity of single cortical neurons and the underlying functional architecture. *Science* 286, 1943–1946 (1999).
25. Sanchez-Vives, M. V., Nowak, L. G. & McCormick, D. A. Cellular mechanisms of long lasting adaptation in visual cortical neurons *in vitro*. *J. Neurosci.* 20, 4286–4299 (2000).
26. Schwindt, P. C., Spain, W. J. & Crill, W. E. Long-lasting reduction of excitability by a sodium-dependent potassium current in cat neocortex neurons. *J. Neurophysiol.* 61, 233–244 (1989).
27. Douglas, R. J., Koch, C., Mahowald, M., Martin, K. A. & Suarez, H. H. Recurrent excitation in neocortical circuits. *Science* 269, 981–985 (1995).
28. Somers, D. C., Nelson, S. B. & Sur, M. An emergent model of orientation selectivity in cat visual cortical cells. *J. Neurosci.* 15, 5449–5465 (1995).
29. Staley, K. J., Longacher, M., Bains, J. S. & Yee, A. Presynaptic modulation of CA3 network activity. *Nat. Neurosci.* 1, 201–209 (1998).
30. Foehring, R. C., Schwindt, P. C. & Crill, W. E. Norepinephrine selectively reduces slow Ca^{2+}- and Na^{+}- mediated K^{+} currents in cat neocortical neurons. *J. Neurophysiol.* 61, 245–256 (1989).
31. Arieli, A., Sterkin, A., Grinvald, A. & Aertsen, A. Dynamics of ongoing activity: explanation of the large variability in evoked cortical responses. *Science* 273, 1868–1871 (1996).
32. Steriade, M., Amzica, F. & Nunez, A. Cholinergic and noradrenergic modulation of slow (approximately 0.3 Hz) oscillation in neocortical cells. *J. Neurophysiol.* 70, 1385–1400 (1993).
33. Lewandowski, M. H., Muller, C. M. & Singer, W. Reticular facilitation of cat visual cortical responses is mediated by nicotinic and muscarinic cholinergic mechanisms. *Exp. Brain Res.* 96, 1–7 (1993).
34. Anderson, J., Lampl, I., Reichova, I., Carandini, M. & Ferster, D. Stimulus dependence of two-state fluctuations of membrane potential in cat visual cortex. *Nat. Neurosci.* 3, 617–621 (2000).
35. Phillis, J. W. Acetylcholine release from the cerebral cortex: its role in cortical arousal. *Brain Res.* 7, 378–389 (1968).
36. Luck, S. J., Chelazzi, L., Hillyard, S. A. & Desimone, R. Neural mechanisms of spatial selective attention in areas V1, V2, and V4 of macaque visual cortex. *J. Neurophysiol.* 77, 24–42 (1997).
37. Mountcastle, V. B., Motter, B. C., Steinmetz, M. A. & Sestokas, A. K. Common and differential effects of attentive fixation on the excitability of parietal and prestriate (V4) cortical visual neurons in the macaque monkey. *J. Neurosci.* 7, 2239–2255 (1987).
38. Goldman-Rakic, P. S. Cellular basis of working memory. *Neuron* 14, 477–485 (1995).
39. Hebb, D. O. *The Organization of Behavior* (John Wiley, New York, 1949).
40. Lorente de No, R. Analysis of the activity of the chains of internuncial neurons. *J. Neurophysiol.* 1, 207–244 (1938).
41. Snodderly, D. M. & Gur, M. Organization of striate cortex of alert, trained monkeys (Macaca fascicularis): Ongoing activity, stimulus selectivity, and widths of receptive field activating regions. *J. Neurophysiol.* 74, 2100–2125 (1995).
42. Ferster, D., Chung, S. & Wheat, H. Orientation selectivity of thalamic input to simple cells of cat visual cortex. *Nature* 380, 249–252 (1996).
43. Reid, R. C. & Alonso, J. M. The processing and encoding of information in the visual cortex. *Curr. Opin. Neurobiol.* 6, 475–480 (1996).
44. Sanchez-Vives, M. V., Nowak, L. G. & McCormick, D. A. Membrane mechanisms underlying contrast adaptation in cat area 17 *in vivo*. *J. Neurosci.* 20, 4267–4285 (2000).